

Electronic Supplementary Information (ESI)

A boron imidazolate framework with mechanochromic and electrocatalytic properties

Tian Wen,^{a, b} Yao Zheng,^a Chaochen Xu,^a Jian Zhang,^b Mietek Jaroniec,^c and Shi-Zhang Qiao*,^a

[a] T. Wen, Dr. Y. Zheng, C. Xu, Prof. S. Z. Qiao
School of Chemical Engineering, The University of Adelaide Adelaide, SA 5005, Australia.
E-mail: s.qiao@adelaide.edu.au

[b] T. Wen, Prof. J. Zhang
State Key Laboratory of Structural Chemistry, Fujian Institute of Research on the Structure of Matter, Chinese Academy of Sciences, Fuzhou, Fujian 350002, P. R. China.

[c] Prof. M. Jaroniec
Department of Chemistry and Biochemistry, Kent State University Kent, OH 44240, USA.

Part I: Experimental Section

1. Single-crystal structural determination

Suitable single crystals of **BIF-89** were carefully selected and glued to a thin glass fiber. Crystallographic data of **BIF-89** were collected on a Mercury single crystal diffractometer equipped with graphite-monochromatic Mo K α radiation ($\lambda = 0.71073 \text{ \AA}$) at room temperature. The structures were solved by direct methods and refined by full-matrix least-squares on F2. Crystal data as well as details of data collection and refinement for **BIF-89** are summarized in Table S1. All powder X-ray diffraction (PXRD) analyses were performed on a Rigaku Dmax2500 diffractometer with Cu K α radiation ($\lambda = 1.54056 \text{ \AA}$) using a step size of 0.05° . Thermogravimetric analyses (TGA) were performed on a Mettler Toledo TGA/SDTA 851e analyzer using a heating rate of $10 \text{ }^\circ\text{C}/\text{min}$ under N₂ atmosphere. Elemental analyses (EA) for C, H, and N were done on an EA1110 CHNSO CE elemental analyzer. Fourier transform infrared (FT-IR) spectra were taken on a Nicolet Magna 750 FT-IR spectrometer in the $4000\text{--}500 \text{ cm}^{-1}$ region by using KBr pellets. Steady-state photoluminescence spectra were recorded by using an Edinburgh FLS920 spectrometer equipped with a continuous Xe 900 xenon lamp.

2. Electrochemical characterization

OER measurements were performed in a three-electrode glass cell. The data were recorded using a CHI760 D bipotentiostat (CH Instruments, Inc., USA). The synthesized samples grown on a substrate (e.g., Ni foam 1cm x1cm) were directly used as the working electrode for electrochemical

characterizations. The reference electrode was Ag/AgCl in 4 M KCl solution and the counter electrode was a platinum wire. The current density was normalized to the geometrical surface area and the measured potentials vs. Ag/AgCl were converted to a reversible hydrogen electrode (RHE) scale according to the Nernst equation ($E_{\text{RHE}} = E_{\text{Ag/AgCl}} + 0.059 \times \text{pH} + 0.205$). A flow of N₂ was maintained over the electrolyte (1.0 M KOH) during electrochemical measurements in order to ensure the O₂/H₂O equilibrium at 1.23 V vs. RHE. The polarization curves were recorded with the scan rate of 5 mVs⁻¹. The working electrodes were scanned for several times before the data for polarization curves were collected, corrected for the iR contribution within the cell. Electrochemical impedance spectroscopy (EIS) measurements were tested by applying an AC voltage with 5 mV amplitude in a frequency range from 100000 to 1 Hz and recorded at 1.60 V vs. RHE.

3. Synthesis of BIF-89

Benzene - 1, 2, 4, 5-tetracarboxylate (0.0165g), CdSO₄·4H₂O (0.0378g), KB(im)₄ (0.0107g), in a N, N-dimethylformamide (DMF; 4mL) / water (H₂O; 1mL) / ethanol (CH₃CH₂OH; 1mL) solution were placed in a 20 mL vial. The sample was heated at 80 °C for 5 days, and then cooled to room temperature. After washing with ethanol and distilled water, the colorless crystals were obtained (31% yield). EA calc. (%) for C₁₇ H₁₅ B Cd N₈ O₅: C, 38.16; H, 2.81; N, 20.95; found: C 38.13, H 2.41, N, 20.97.

4. Electrocatalysts synthesis

4.1 Synthesis of BIF-89-NF-1

Firstly, a Ni foam (1.5 cm × 2cm × 0.02 cm) was repeatedly rinsed with absolute ethanol and Milli-Q water through ultrasonication treatment and was placed in a 20 mL vial. Secondly, benzene - 1, 2, 4, 5-tetracarboxylate (0.0265g), CdSO₄·4H₂O (0.0478g), and KB(im)₄ (0.0227g) with a N, N-dimethylformamide (DMF; 4mL) / water (H₂O; 1mL) / ethanol (CH₃CH₂OH; 1mL) solution were added into the vial above, which was heated at 80 °C for 48 hours, and then cooled down to room temperature at a rate of 5°C h⁻¹. The Ni foil with attached microcrystalline BIF-89 (**BIF-89-NF-1**) was successively washed with H₂O and methanol before immersing it in Fe(NO₃)₃ (10 mM) solution for one hour. Further, the obtained **Fe@BIF-89-NF-1** was washed with water three times before use.

4.2 Synthesis of BIF-89-NF-2

The procedure for fabrication of **BIF-89-NF-2** was the same as that for **BIF-89-NF-1** except for prolonging reaction time to 5 days. **BIF-89-NF-2** was successively washed with H₂O and methanol before immersing it in Fe(NO₃)₃ (10 mM) solution for one hour. Further, the obtained **Fe@BIF-89-NF-2** was washed with water three times before use.

4.3 Synthesis of BIF-89@CP

The procedure for fabrication of **BIF-89@CP** was the same as that for **BIF-89-NF-1** except for using carbon paper instead of the Ni foam.

4.4 Synthesis of Fe@BIF-89@CP

The procedure for preparation of **Fe@BIF-89@CP** was the same as that for **Fe@BIF-89-NF-1** except for using **BIF-89@CP** instead of **BIF-89-NF-1**.

4.5 BIF-89 coated on glassy carbon electrode (BIF-89@GC)

The as-synthesized **BIF-89** was ultrasonically dispersed in the mixture of 1 mL of Milli-Q water and ethanol, and then transferred onto the glassy carbon electrode with a loading amount of ~ 0.2 mg cm⁻². The resulting electrode was subjected to overnight solvent evaporation in air, subsequent coating with a thin layer of Nafion solution (1.0 wt.% water solution), and drying in air for another 1 h.

4.6 Fe@BIF-89 coated on glassy carbon electrode (Fe@BIF-89@GC)

The procedure for preparation of **Fe@BIF-89@GC** was the same as that for **BIF-89@GC** except for using **Fe@BIF-89** instead of **BIF-89**.

Part II: Supplementary Results

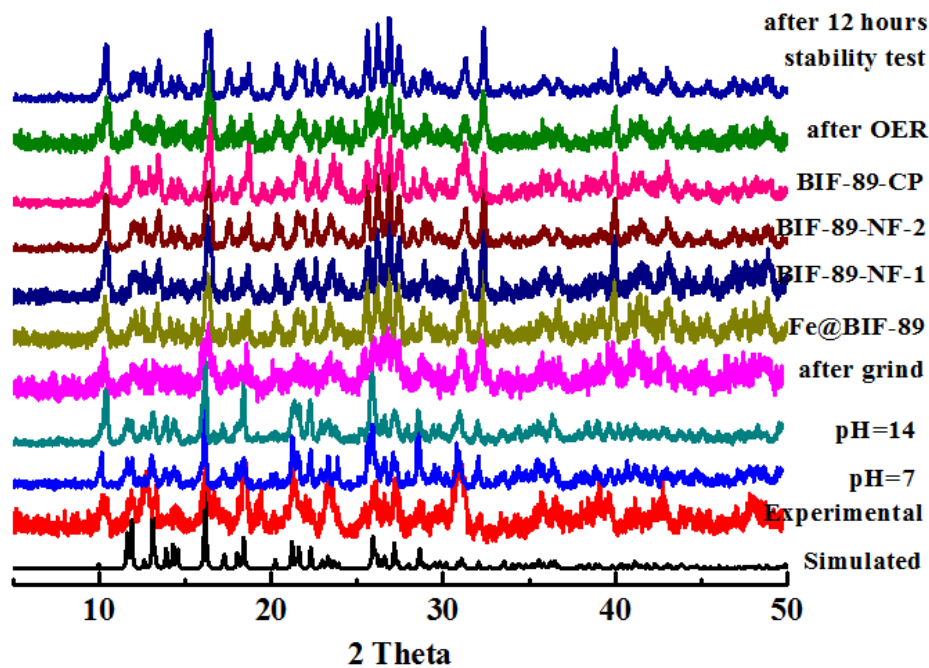


Figure S1. The XRD patterns of BIF-89 under different conditions.

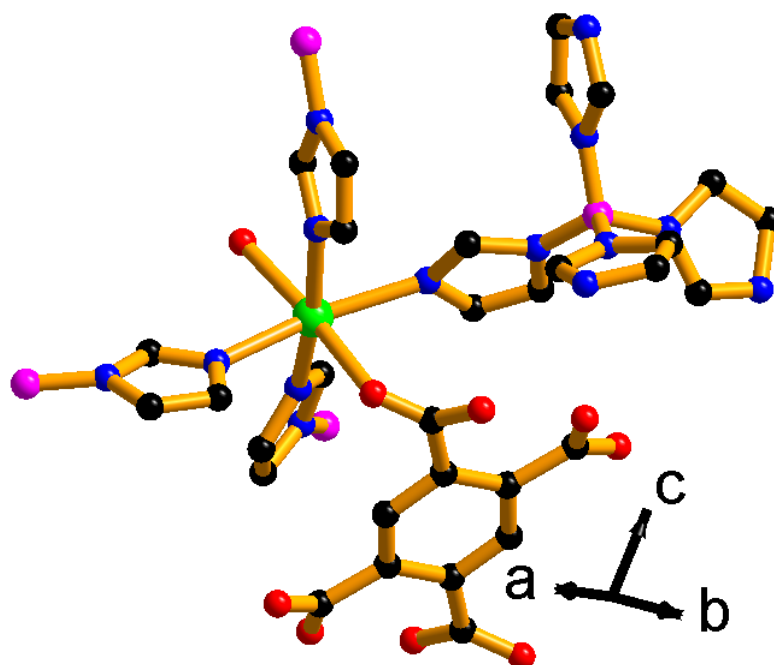


Figure S2. The coordination environment of BIF-89.

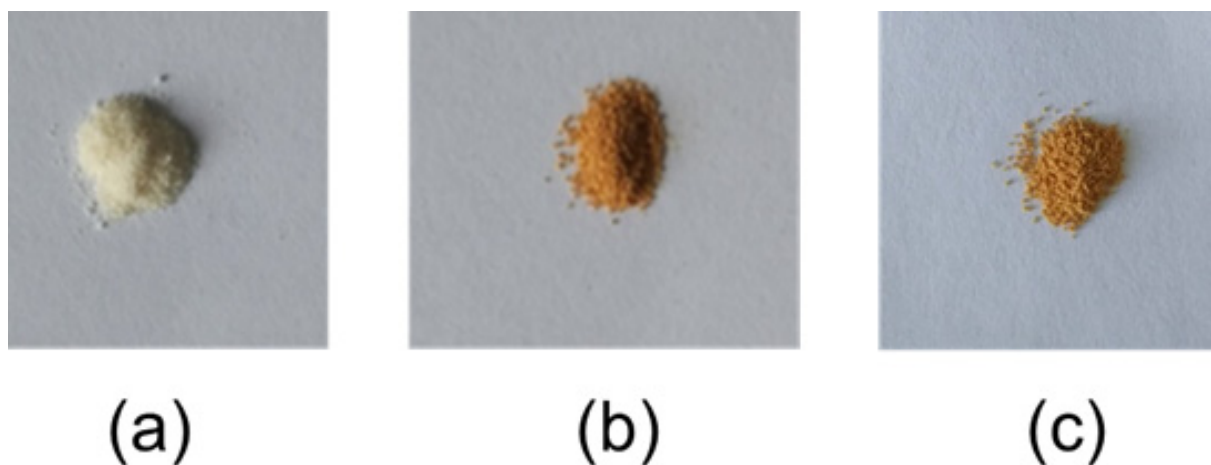


Figure S3. (a) Optical image of **BIF-89**; (b) optical image of **Fe@BIF-89**; (c) optical images of **Fe@BIF-89** after immersing in water for 24 hours.

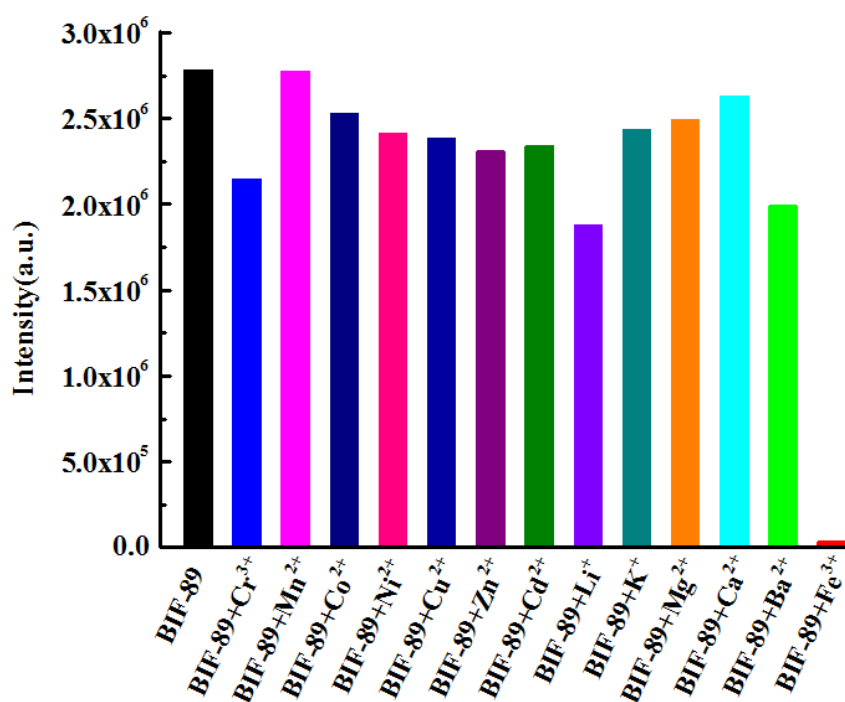


Figure S4. Fluorescence response of **BIF-89** in the various metal ion aqueous solutions (10 mM) at 360 nm. The metal salts listed below were used in the luminescent sensing experiments: $\text{Fe}(\text{NO}_3)_3$, $\text{Cr}(\text{NO}_3)_3$, $\text{Mn}(\text{NO}_3)_2$, $\text{Co}(\text{NO}_3)_2$, $\text{Ni}(\text{NO}_3)_2$, $\text{Cu}(\text{NO}_3)_2$, $\text{Zn}(\text{NO}_3)_2$, $\text{Cd}(\text{NO}_3)_2$, LiNO_3 , KNO_3 , $\text{Mg}(\text{NO}_3)_2$, $\text{Ca}(\text{NO}_3)_2$, $\text{Ba}(\text{NO}_3)_2$. The dried and fresh sample of **BIF-89** (10.00 mg) in 10 mL of H_2O was firstly ultrasonicated for one hour to obtain the aqueous colloidal white suspension of **BIF-89**. The sensing experiments were carried out by adding 20 mL of aqueous solutions of different metal ions to 2 mL of **BIF-89** water solution and measuring the photoluminescence spectra.

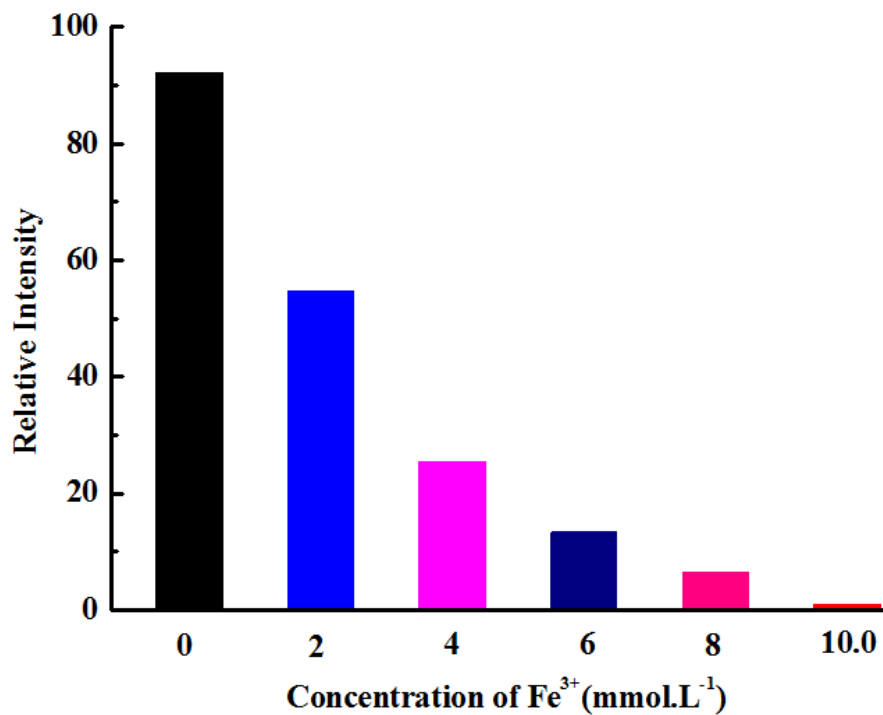


Figure S5. Emission spectra of Fe@BIF-89 at different concentrations of Fe³⁺.

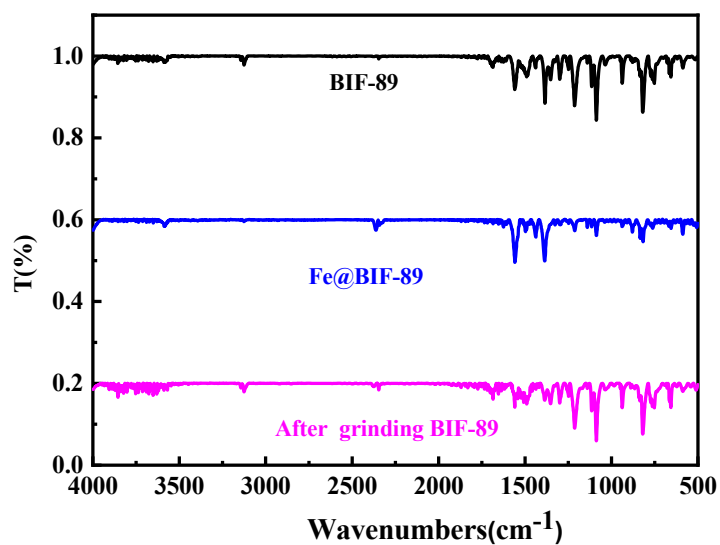


Figure S6. Infrared spectra of BIF-89, Fe@BIF-89 and BIF-89 after grinding.

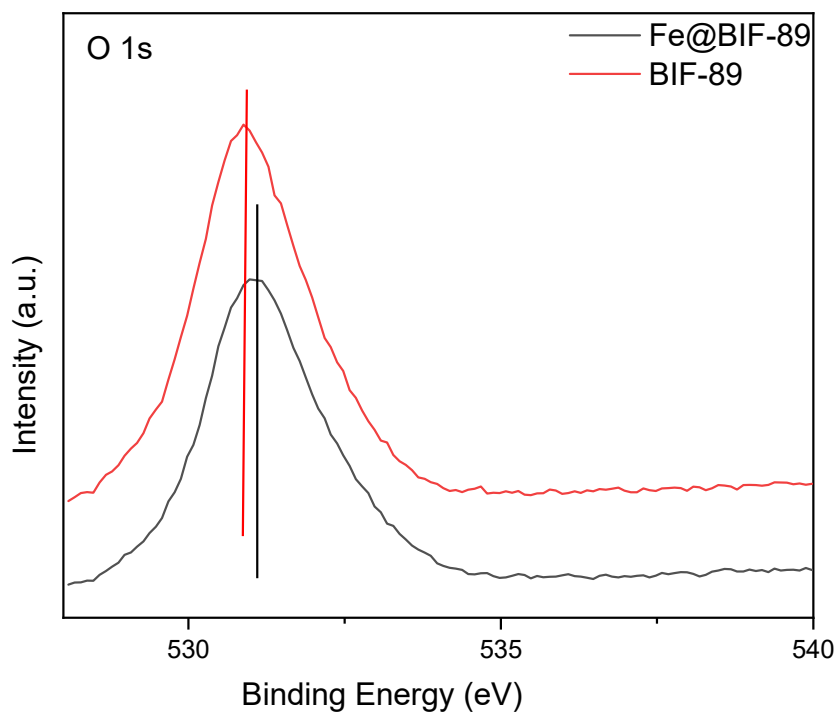


Figure S7. O1s XPS spectrum of **BIF-89** and **Fe@BIF-89** samples.

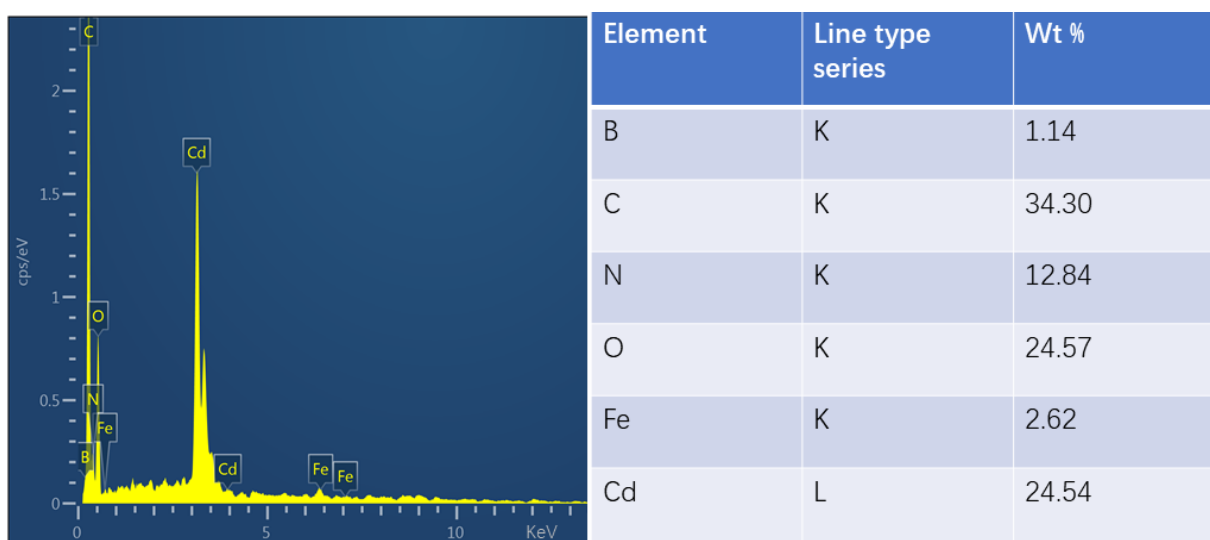


Figure S8. EDX analysis of **Fe@ BIF-89**.

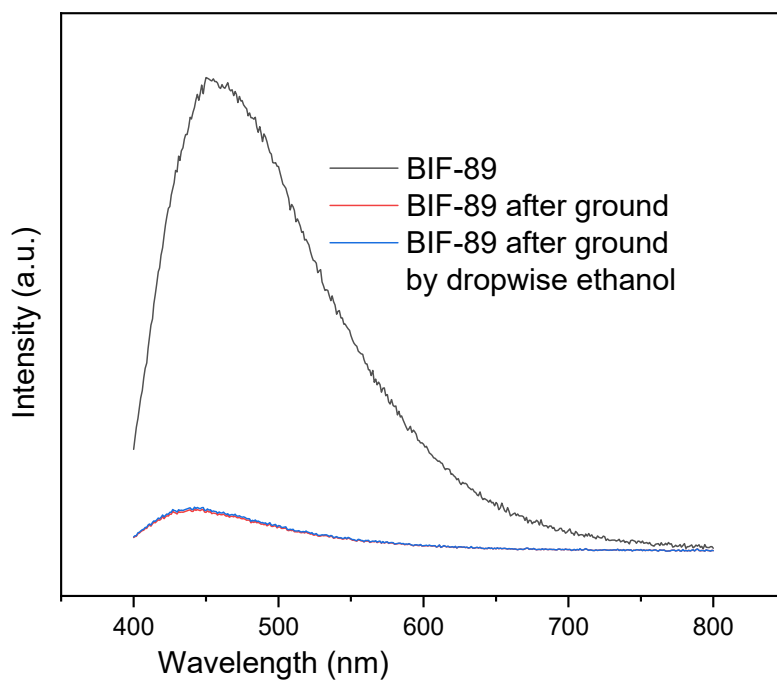


Figure S9. The solid-state emission spectra of BIF-89 at different conditions.

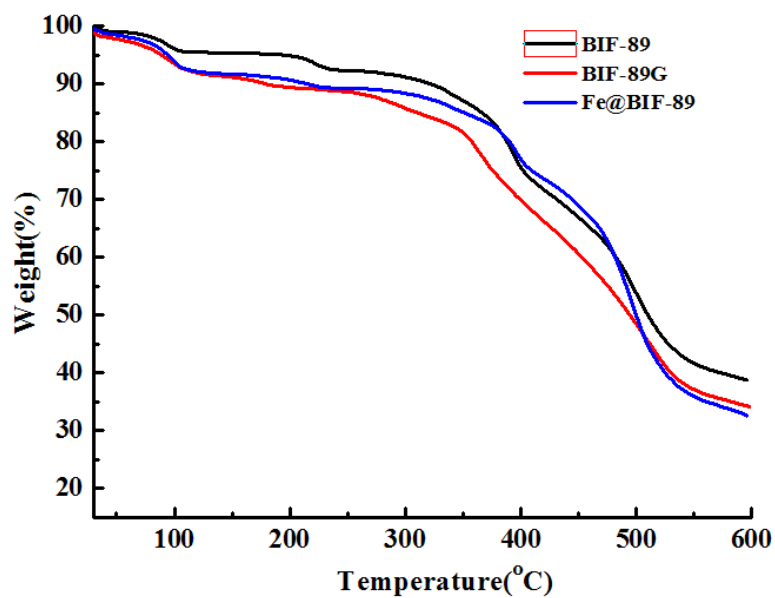


Figure S10. Thermogravimetric profiles recorded for **BIF-89**, **BIF-89** after grinding (**BIF-89 G**) and **Fe@BIF-89**.

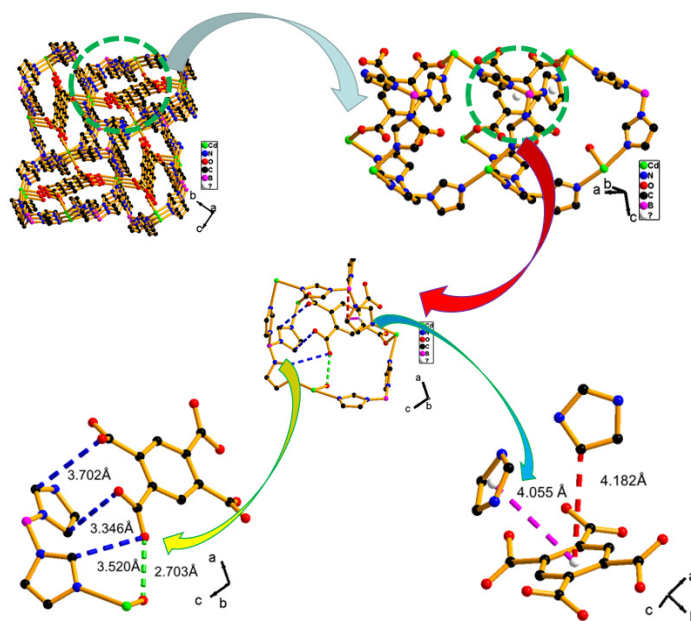


Figure S11. Some weak interactions among btc and imidazolate ligands and the coordinated water molecules.

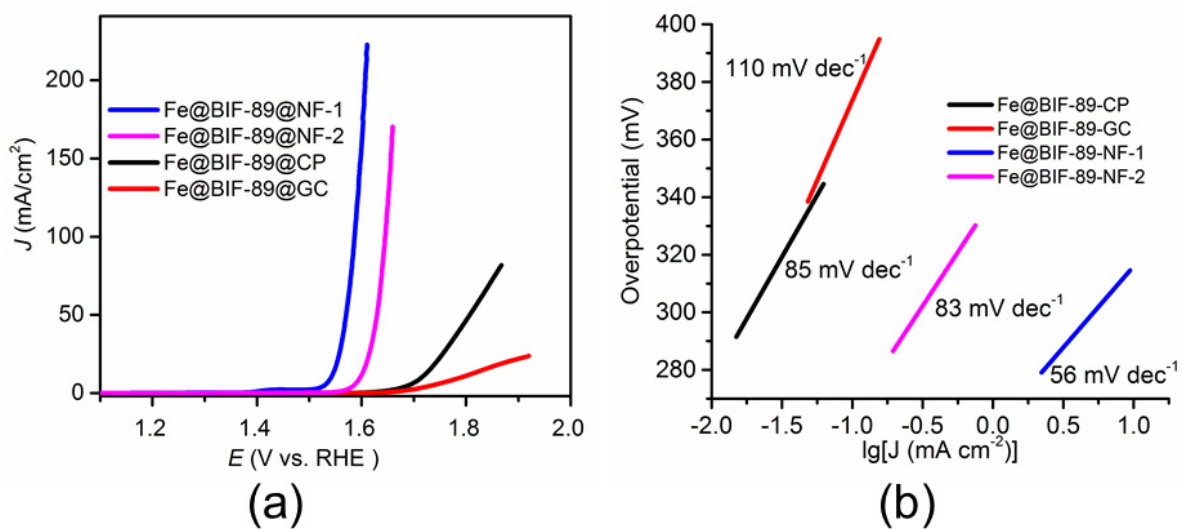


Figure S12. LSV and Tafel plots for **Fe@BIF-89** on various substrates in 1M KOH aqueous solution.

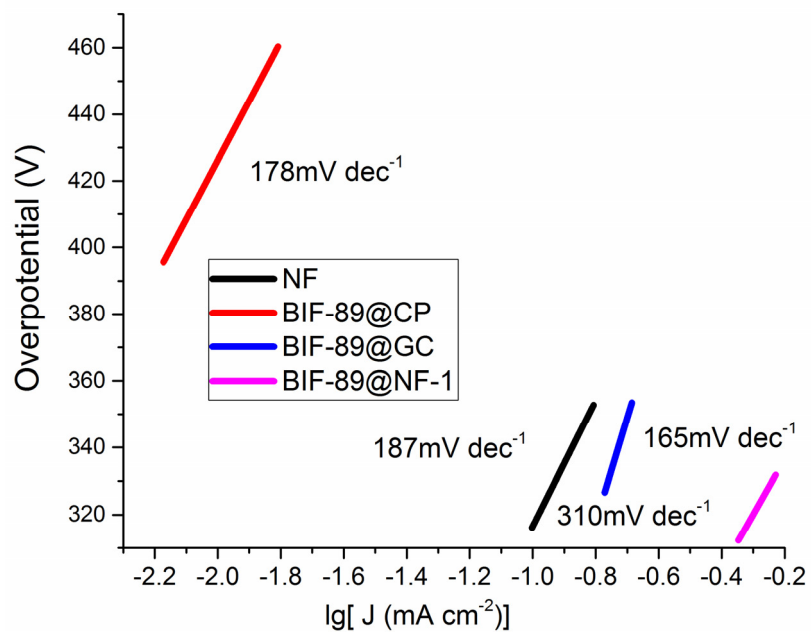


Figure S13 Tafel plots for **BIF-89** on various substrates and pure Ni foam at pH = 14.

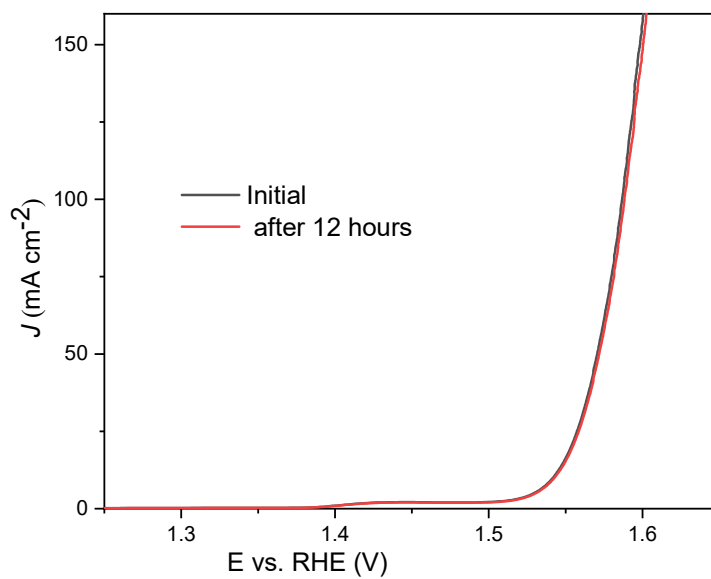


Figure S14. LSV curves measured for Fe@BIF-89 before and after stability test.

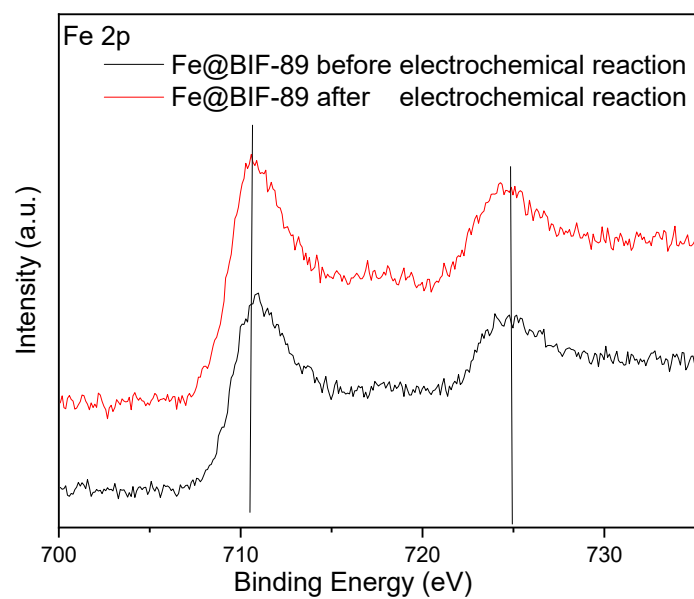


Figure S15. Fe2p XPS spectrum of **Fe@BIF-89** before and after electrochemical reaction.

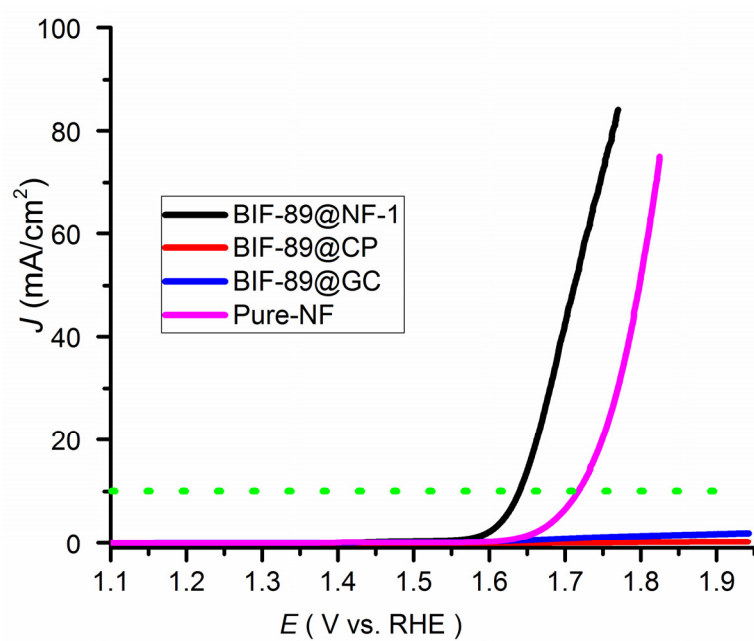


Figure S16. LSV curves measured for **BIF-89** on various substrates and pure Ni foam at pH = 14.

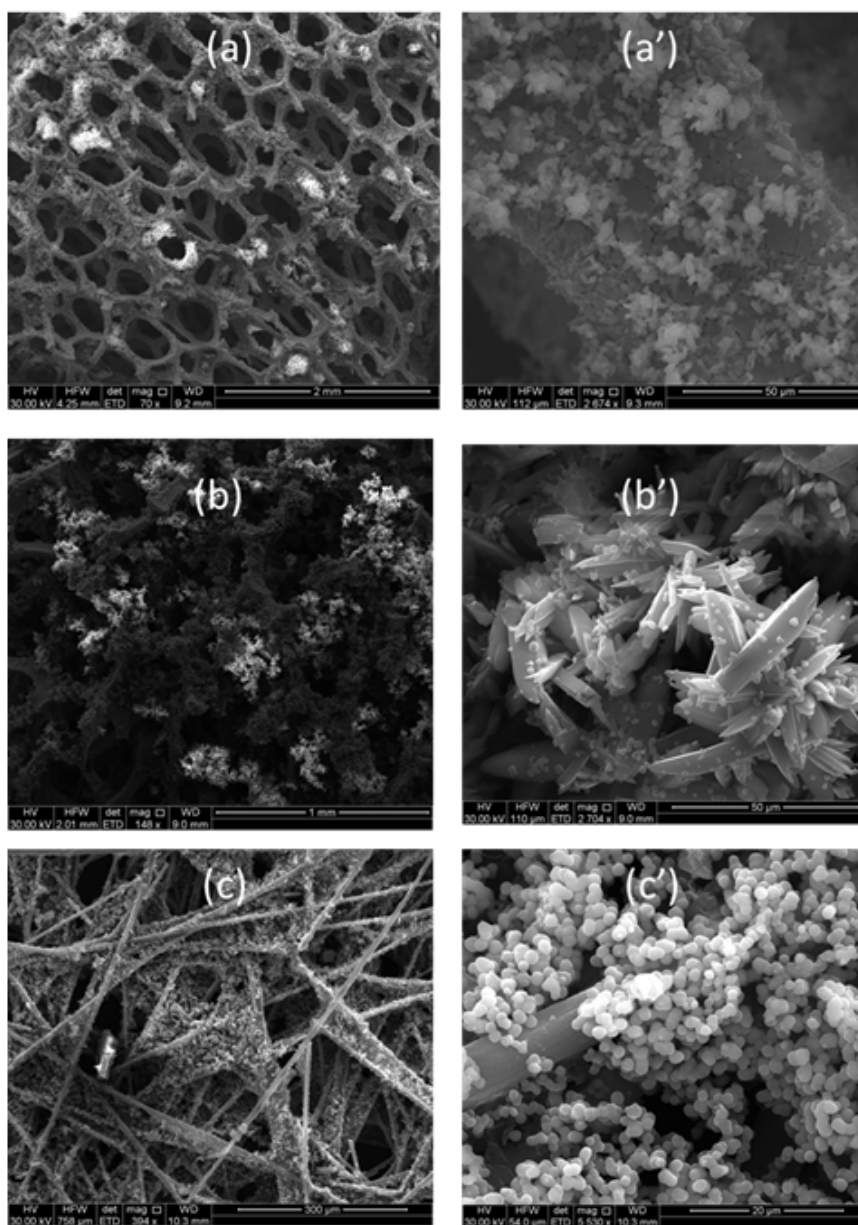


Figure S17. SEM images of (a) **BIF-89-NF-1** (mass loading 0.19 mg cm^{-2}), (b) **BIF-89-NF-2** (mass loading 0.31 mg cm^{-2}) and (c) **BIF-89-CP** (mass loading 0.08 mg cm^{-2}). The different morphologies, mass loading and conductive substrate affect the OER performance.

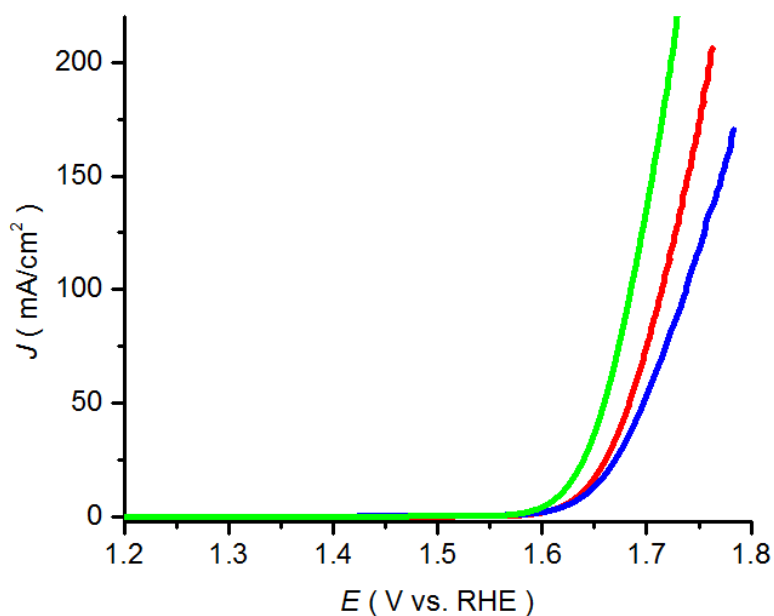


Figure S18. LSV curves measured for **Fe@BIF-89-NF-1** at $\text{pH} = 14$. The as-synthesized **BIF-89-NF-1** was washed with H_2O and methanol before immersing it in $\text{Fe}(\text{NO}_3)_3$ (10 mM) solution for 15 mins, 10 mins, and 1 min. The resulting electrode was subjected to overnight solvent evaporation in air and drying in air for another 4 h (green: 1.8%, red: 1.1%, blue: 0.5%, Fe^{3+} uptake was determined by ICP).

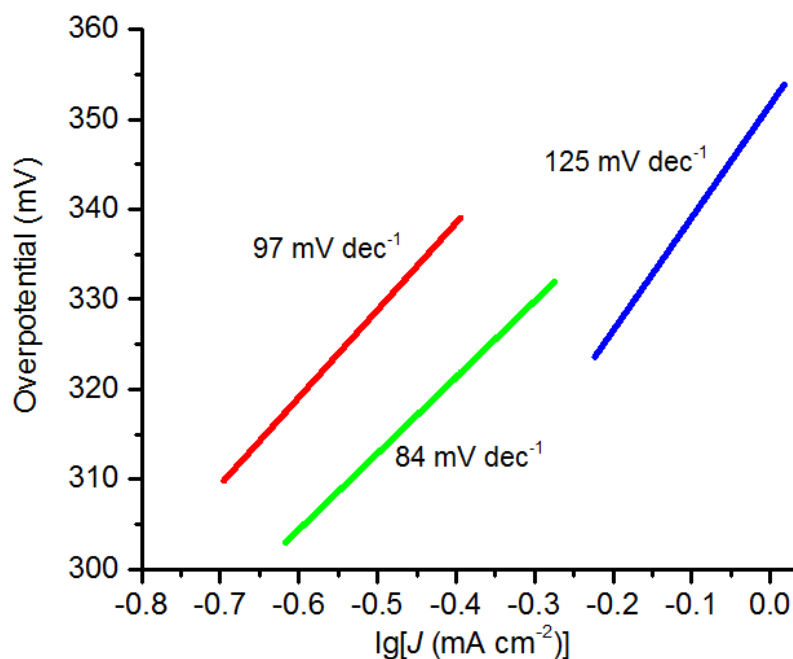


Figure S19. Tafel plots for **Fe@BIF-89-NF-1** at $\text{pH} = 14$.

Table S1. Summary of Crystallographic Data and Refinement Results

	BIF-89
chemical formula	C ₁₇ H ₁₅ B Cd N ₈ O ₅
formula mass	535
Space group	P 21/c
a/Å	9.2198(5)
b/Å	14.0236(8)
c/Å	15.7941(8)
α/°	90.00
β/°	105.723(5)
γ/°	90.00
Volume/Å ³	1965.69(19)
Z, calculated density(g/cm ³)	4, 1.806
absorption coefficient (mm ⁻¹)	1.162
F(000)	1064.0
R _{int}	0.0398
GOF on F ₂	1.0
R ₁ , ^a wR ₂ [I > 2δ(I)]	R ₁ = 0.0314, wR ₂ = 0.0652
R ₁ , wR ₂ (all data)	R ₁ = 0.0421, wR ₂ = 0.0694
CCDC Number	1584142

$$^a R_1 = \Sigma(|F_o| - |F_c|)/\Sigma|F_o|, wR_2 = [\Sigma w(F_o^2 - F_c^2)^2/\Sigma w(F_o^2)^2]^{0.5}$$

Table S2 Inductively Coupled Plasma Emission-Mass Spectrometry

Sample	Fe (ppb)	Cd(ppb)	Fe content	Cd content
Fe@ BIF-89	59.80	2658.59	2.3%	97.8%

Table S3. The solid-state photoluminescent lifetimes (τ) of the **BIF-89** sample before and after grinding.

T (K)	τ_1 (s) (%)	τ_2 (s) (%)	τ_3 (s) (%)
77 K	8.284E-10 (38.50)	5.463E-9 (38.61)	6.367E-8 (22.90)
298 K	2.195E-10 (40.72)	4.857E-9 (27.14)	5.873E-8 (32.14)
77 K Ground	1.057E-10 (59.27)	1.907E-8 (23.98)	9.690E-8 (16.75)
29 K Ground	7.855E-11 (56.97)	2.461E-8 (27.51)	1.303E-7 (15.52)

Table S4. Comparison of the OER activities of **Fe@BIF-89-NF -1** with the reported MOF-based electrocatalysts.

Catalyst	Onset potential (V vs. RHE)	Potential at 10 mA cm ⁻² (mV vs. RHE)	Tafel Slope (mV dec ⁻¹)	Mass loading (mg cm ⁻²)	Substrate	Ref
MAF-X27-OH pH=14	1.47	292	88	1.13	Cu Foil	1
Fe ₃ -Co ₂ pH=13	1.431	237	79	0.2	Cu Foil	2
Co-ZIF-9 pH=13	NA	510 (1 mA cm ⁻²)	193	0.15	FTO glass	3
Co-WOC-1 pH=13	1.62	390 (1 mA cm ⁻²)	128	0.28	GC	4
FeTPyP-Co pH=13	1.47	351 (1 mA cm ⁻²)	NA	NA	Au	5
USTA-16 pH=14	1.60	408	77	0.35	GC	6
NiCo-UMOFN pH=14	1.39	189	NA	0.2	Cu Foil	7

Co/MIL-100(Fe) pH=13	1.58	734 (5mA cm ⁻²)	NA	0.24	GC-RDE	8
Ni/Fe-BTC pH=13	NA	270	43	0.5	NF	9
Co/MIL-101(Cr)-O pH=13	1.53	477	122	0.5	GC-RDE	10
UiO-67-[RuOH ₂] pH=6.2	1.96	818 (0.15 mA cm ⁻²)	NA	0.07	FTO	11
Fe LDHs	NA	258	53	NA	NF	12
FeOx	NA	431	93	NA	CFC	13
FeOx/CFC-4	NA	371	50	NA	CFC	13
FeOx/CFC-6	NA	389	NA	0.124	CFC	13
FeOx/CFC-8	NA	401	NA	NA	CFC	13
NiFe NS	NA	340	61	NA	NF	14
NiFe NS	NA	300	40	0.07	GC	15
b-NiFe LDH	NA	459	62	0.25	GC	16
b-NiFe LDH+NGF	NA	392	52	0.25	GC	16
n-NiFe LDH/GF	NA	372	58	0.25	GC	16
n-NiFe LDH /NGF	NA	337	45	0.25	GC	16
m-NiFe/CNx	NA	360	59.1	0.25	GC	17
Fe@BIF-89-NF-1 pH=14	1.49	312	56	0.18	NF	This work

References:

- [1] X.-F. Lu, P.-Q. Liao, J.-W. Wang, J.-X. Wu, X.-W. Chen, C.-T. He, J.-P. Zhang, G.-R. Li, X.-M. Chen, *J. Am. Chem. Soc.*, **2016**, *138*, 8336.
- [2] J.-Q. Shen, P.-Q. Liao, D.-D. Zhou, C.-T. He, J.-X. Wu, W.-X. Zhang, J.-P. Zhang, X.-M. Chen, *J. Am. Chem. Soc.*, **2017**, *139*, 1778.
- [3] S. Wang, Y. Hou, S. Lin, X. Wang, *Nanoscale*, **2014**, *6*, 9930.
- [4] P. Manna, J. Debgupta, S. Bose, S. K. Das, *Angew. Chem. Int. Ed.*, **2016**, *55*, 2425.
- [5] B. Wurster, D. Grumelli, D. Hötger, R. Gutzler, K. Kern, *J. Am. Chem. Soc.*, **2016**, *138*, 3623.
- [6] J. Jiang, L. Huang, X. Liu, L. Ai, *ACS Appl. Mater. Inter.*, **2017**, *9*, 7193.
- [7] S.-L. Zhao, Y. Wang, J.-C. Dong, C.-T. He, H.-J. Yin, P.- F. An, K. Zhao, X.-F. Zhang, C. Gao,

- L.-J. Zhang, J.-W. Lv, J.-X. Wang, J.-Q. Zhang, A. M. Khattak, N. A. Khan, Z.-X. Wei, J. Zhang, S.-Q. Liu, H.-J. Zhao, Z.-Y. Tang, *Nat. Energy*, **2016**, 1, 16184.
- [8] H. Wang, F. Yin, G. Li, B. Chen and Z. Wang, *Int. J. Hydrogen Energy*, **2014**, 39, 16179.
- [9] L. Wang, Y.-Z. Wu, R. Cao, L.-T. Ren, M.-X. Chen, X. Feng, J.-W. Zhou, B. Wang, *ACS Appl. Mater. Interfaces*, **2016**, 8, 16736.
- [10] X.-B. He, F.-X. Yin, G.-R. Li, *Int. J. Hydrogen Energy*, **2015**, 40, 9713.
- [11] B. A. Johnson, A. Bhunia, S. Ott, *Dalton Trans.* **2017**, 46, 1382.
- [12] J. Chi, H. M. Yu, B. W. Qin, L. Fu, J. Jia, B. L. Yi, Z. G. Shao, *ACS Appl. Mater. Interfaces*, 2017, 9, 464.
- [13] F. Yan, C. Zhu, S. Wang, Y. Zhao, X. Zhang, C. Li, Y. Chen, *J. Mater. Chem. A*, **2016**, 4, 6048.
- [14] X. Lu, C. Zhao, *Nat. Commun.* **2015**, 6, 6616.
- [15] F. Song, X. Hu, *Nat. Commun.* **2014**, 5, 4477.
- [16] C. Tang, H. Wang, H. Wang, Q. Zhang, G. Tian, J. Nie, F. Wie, *Adv. Mater.* **2015**, 27, 4516.
- [17] S. Q. Ci, S. Mao, Y. Hou, S. M. Cui, H. J. Kim, R. Ren, Z. H. Wen, J. H. Chen. *J. Mater. Chem. A*, **2015**, 3, 7986.